Hindawi
Journal of Chemistry
Volume 2024, Article ID 5580782, 9 pages
https://doi.org/10.1155/2024/5580782

Research Article

Fabrication of Silk Fibroin Film with Strong Anticoagulant Property from the Synergy of Deep Eutectic Solvents and UV-Light Irradiation

Chunyan Yu, Meiling Pu, Qiuyang Chen, Shitao Yu, and Lu Li

State Key Laboratory Base of Eco-Chemical Engineering, College of Chemical Engineering, Qingdao University of Science and Technology, Qingdao 266042, China

Correspondence should be addressed to Lu Li; zhanglilu@126.com

Received 9 July 2023; Revised 9 November 2023; Accepted 20 November 2023; Published 22 January 2024

Academic Editor: Josefina Pons

As a biological macromolecule, silk fibroin (SF) has great application potential in anticoagulant. However, its complex molecular structure leads to its poor solubility, which limits the application of SF. In this study, a novel SF film with strong anticoagulant properties was fabricated through the synergistic effect of LiBr deep eutectic solvents (DESs) and UV-light irradiation. Under the optimum conditions, the plasma recalcification time of SF film was 182 s, the hemolysis rate was 3.93%, and the dynamic coagulation time remained at a high level up to 60 min. The synergistic effect of UV-light and DES can promote the enhancement of hydrophilicity and the decrease of surface roughness of SF films, and thus the anticoagulant properties of the films were enhanced. The structure change, wettability, and roughness of SF films were characterized by XRD, FTIR, contact angle, and AFM. In the meantime, the wavelength of the UV-light and the irradiation time have an effect on the anticoagulant properties of the SF films. Furthermore, the improvement of the anticoagulant properties of SF films exhibits good universality for different LiBr DESs. The study provides a new direction for the preparation of strong anticoagulation SF films, as well as its application in life sciences.

1. Introduction

Anticoagulant materials have been widely used in artificial vessels [1], artificial hearts [2], and medication of disseminated intravascular coagulation and thrombosis [3]. The excellent anticoagulant properties are an important basis to judge whether the material can be used in organisms [4]. Therefore, it is highly desirable to prepare a material with excellent anticoagulant properties. At present, most anticoagulant materials improve their anticoagulant properties by adding heparin, but its price is relatively high and the continuous administration of heparin may lead to systemic bleeding risk [5].

SF films, with nontoxic, nonallergenic, and nonirritating properties, favorable biocompatibility, biodegradability, and minimal immunogenicity, are promising natural polymer materials for the preparation of anticoagulant materials [6, 7]. However, there are some deficiencies in the preparation of SF films at present, such as the solvent problem. In the traditional SF film making process, most of the solvents used are inorganic salt solutions [8], which are highly toxic [9] and difficult to recover [10], and the process is cumbersome and it takes a long time for dialysis after the dissolution [11]. The anticoagulant properties of the materials can be affected by solvents because the hydrophilicity of the materials can be affected by solvents. The anticoagulant properties are affected by the hydrophilicity of the materials, and usually, high hydrophobicity leads to weak anticoagulant properties [12, 13]. Therefore, in order to obtain SF films having strong anticoagulant properties, it is necessary to improve hydrophilicity of SF films. As a new type of green solvent, DES has the advantages of thermal stability, easy biodegradation, good biocompatibility, simple synthesis operation, and nontoxic [14, 15], and it has been reported that DES can improve the hydrophilicity of the materials [16]. Hence, we chose DES as a solvent to dissolve SF instead

of inorganic salt solutions and tried to improve the hydrophilicity of SF, thus enhancing the anticoagulant properties of SF.

In addition, the anticoagulant properties of the materials can also be affected by UV-light. Fadel et al. [17] studied the effect of UV-light irradiation on the surface properties and anticoagulant properties of poly(terephthalic acid). The results showed that the wettability and anticoagulant properties of the polymer were enhanced. For SF, UV-light can change the secondary structure of SF, and then hydrophilicity of SF can be affected [18, 19]. At the same time, UV-light can also affect the roughness of the materials [20]. Usually, high roughness usually leads to weak anticoagulant properties [21]. Therefore, we tried to couple UV-light to the dissolution process of SF, and anticoagulant properties of SF films were enhanced through the synergistic effect of UV-light and DES.

In this study, DES was used as a solvent to obtain a homogenous SF solution under UV-light irradiation. The effect of DES and light on the hydrophilicity and roughness of SF films was related to the film anticoagulant properties. The causes of the changes of anticoagulant properties were analyzed by XRD, FTIR, contact angle, and AFM. Also, the effects of different DESs on anticoagulant properties of SF films were analyzed.

2. Materials and Methods

2.1. Materials. $NaHCO_3$ was purchased from Tianjin Dingshengxin Chemical Co. Ltd. LiBr, $ZnCl_2$, $(NH_4)_2SO_4$, and NaCl were purchased from Sigma Chemical Reagent Co. Ltd. $CaCl_2$ was purchased from Shanghai Macklin Biochemical Co. Ltd. Triethoxyvinylsilane was purchased from Jiuding chemistry. H_2SO_4 and H_2O_2 were purchased from Tianjin Bodi Chemical Co. Ltd. C_2H_5OH was purchased from Tianjin BASF Chemical Trade Co. Ltd. CH_3COOH was purchased from Kaifeng Chemical Reagent Factory. The above chemicals were of analytical grade without further purification. *Bombyx mori* silkworm cocoon was purchased from Tongxiang Daopu silk Co. Ltd. The fresh rabbit blood was purchased from Qingdao topson Biotechnology Co. Ltd.

2.2. Preparation of SF Films in LiBr/$ZnCl_2$ DES under Non-Light Irradiation. LiBr/$ZnCl_2$ DES was prepared with the molar ratio of LiBr to $ZnCl_2$ of 2 : 1. LiBr and $ZnCl_2$ with a total mass of 10 g were weighed and transferred to a 100 mL three-necked flask at 120 C. 10 mL deionized water was added and stirred well before the dissolution of SF, and then the degummed SF was added to the flask in amounts of 0.1 g at a time, with more only added after the previously added SF was completely dissolved. Finally, SF with a total mass of 1.0 g was dissolved. The SF solution was placed on a special flat glass plate while it was hot, coated evenly, placed for half an hour, and naturally cooled at room temperature. After that, the glass plate was put into a tray containing 10% aqueous solution of $(NH_4)_2SO_4$ and solidified for about 2 h. Subsequently, SF films were washed with deionized water for several times and dried at 60°C in oven. When the SF films began to separate from the surface of the glass plate, it indicated that the films have been completely dried. The prepared SF films were peeled from the glass plate carefully to obtain the final product of SF films.

2.3. Preparation of SF Films in LiBr/Urea DES under Non-Light Irradiation. LiBr/urea DES was prepared with the molar ratio of LiBr to urea of 1 : 1. LiBr and urea with a total mass of 10 g were weighed and transferred to a 100 mL three-necked flask at 100°C. 10 mL deionized water was added and stirred well before the dissolution of SF, and then the degummed SF was added to the flask in amounts of 0.1 g at a time, with more only added after the previously added SF was completely dissolved. Finally, SF with a total mass of 0.8 g was dissolved. The others were the same as those of LiBr/$ZnCl_2$ DES.

2.4. Preparation of SF Films under Light Irradiation. The preparation of DES was the same as that of non-light irradiation. After DES was heated and dissolved, 10 mL deionized water was added and stirred well. Subsequently, SF was further heated and dissolved by heating jacket under different UV-light conditions (Table 1). The others were the same as those of non-light irradiation.

2.5. Characterizations of SF Films

2.5.1. Surface Micromorphology. The surface roughness of SF films was observed by atomic force microscope (AFM, MultiMode 8). The films were cut into square pieces 5 mm × 5 mm in size and stuck on the circular stage with special double-sided adhesive tape. The sample and the carrier piece were put on the sample platform using the forceps provided by the instrument. The sample area was carefully adjusted and moved to the middle position. It should be noticed that the probe and laser source should not be touched. The software was operated and the needle was automatically finished. Subsequently, the probe was dropped to the detection distance and the "scanning" button was pressed to start scanning the sample.

2.5.2. Determination of Wettability of SF Films. The wettability of SF films was measured by static water contact angle. The SF films were cut into proper size with scissors and fixed on the sample slide. The spacing was fine adjusted and the nut on the measuring instrument was rotated so that the water drops can be accurately dropped on the sample film from the needle head. The degree of static contact angle was calculated using the analysis system until the state of water droplet on the film is stable and no longer changes. For each sample, three positions were selected for measurement, and the average value was taken.

2.5.3. Determination of SF Film Structure. Fourier-transform infrared spectroscopy (FTIR) of SF films was performed using a Nicolet 510P infrared spectrometer. FTIR measurements of samples were recorded between

Table 1: Different UV-light conditions.

Wavelength (nm)	Distance (cm)	Time (h)
254	11	5
		6
295		6
365		5

4000 cm^{-1} and 400 cm^{-1}. The SF films prepared under non-light and light irradiation conditions were tested, and the structural change after light irradiation was analyzed.

X-ray diffraction (XRD) measurements were performed using a D/max-rB rotary X-ray powder diffractometer (Rigaku, Tokyo, Japan): CuK target, $A = 0.115418$ nm with step width of 0.02, diffraction rate of 2°/min, and diffraction range of 5° to 80°. The SF films prepared under non-light and light irradiation conditions were tested, and the structural change after light irradiation was analyzed.

2.6. Hemocompatibility of SF Films. Hemocompatibility of SF films was evaluated by plasma recalcification assay, dynamic coagulation assay, and hemolysis assay. The normal physiological activities of the material will not be affected after contacting with blood, which indicates that the material has excellent hemocompatibility.

2.6.1. Silane Treatment of Test Tube. The test tube was cleaned as follows: a sufficient amount of piranha solution was prepared by mixing concentrated sulfuric acid and 30% hydrogen peroxide with 2 : 1 volume ratio [22]. The glass tube was immersed into the piranha solution and heated at 80°C for 45 min. The test tube was taken out, washed with distilled water for several times, and cleaned in an ultrasonic device for 10 min, and then the test tube was washed with absolute ethanol three times, cleaned in an ultrasonic for 10 min, and dried in an oven at 110°C. The cleaned test tube was put into 95% ethanol solution containing 5% triethoxyvinylsilane and 0.5% anhydrous acetic acid and reacted for 20 min at room temperature. Before use, 5% triethoxyvinylsilane was hydrolyzed overnight in 95% ethanol solution containing 0.5% glacial acetic acid. After the reaction, the test tube was washed with absolute ethanol three times, cleaned in an ultrasonic for 10 min, and dried in an oven at 110°C.

2.6.2. Plasma Recalcification Time. Plasma recalcification time is a common method to evaluate the anticoagulant properties of materials in vitro. When Ca^{2+} is added to platelet-poor plasma, the blood coagulation process caused by endogenous coagulation factors occurs again, and the soluble fibrinogen becomes an insoluble fibrin polymer. The time required for this process is the plasma recalcification time. The SF films were cut into 2 mm × 2 mm in size and put into a test tube containing 200 μL platelet-poor plasma. The test tube was placed in the constant temperature bath at 37°C for 10 min, and 0.1 mL of $CaCl_2$ (0.025 mol/L) solution was added at the same temperature. The time when a filament appeared in the test tube was the plasma recalcification time. Three parallel samples were set for each group, and the average value of the results was taken [23].

2.6.3. Dynamic Coagulation Time. In vitro dynamic coagulation time can be used to detect the level of coagulation factor activation and to evaluate the effect of the tested substance on the coagulation time. The higher the BCI value, the stronger ability of the material to inhibit thrombosis. The SF films were cut into 5 mm × 5 mm in size and rinsed in physiological saline at 37°C. After that, the films were put into the bottom of silylation test tube, and 0.1 mL of anticoagulated rabbit whole blood was added. Subsequently, the test tube was put into constant temperature water bath at 37°C. After 1 min, 25 μL $CaCl_2$ (0.1 mol/L) aqueous solution was dripped, and the mixture was shaken to uniformly mix $CaCl_2$ and blood. The prepared samples were placed in the constant temperature bath at 37°C for 5 min, 10 min, 20 min, 40 min, and 60 min. The test tube was taken out and a volume of 30 mL of deionized water was added. The absorbance of these solutions was measured at 545 nm [24]. The blood anticoagulant index (BCI) was calculated as follows:

$$\mathrm{BCI} = \frac{\mathrm{As}}{\mathrm{Aw}} \times 100\%, \quad (1)$$

where Aw denotes the absorbance of mixture of 30 mL deionized water and 0.1 mL anticoagulated rabbit whole blood and As denotes the absorbance of test samples.

2.6.4. Hemolysis Assay. The normal physiological activities of blood will not be affected after contacting with blood, which indicates that the material has excellent hemocompatibility. Only when the hemolysis rate of biofilms is no more than 5%, can it meet the medical requirements. Hemolysis was evaluated by fresh rabbit whole blood under static condition. Fresh anticoagulated rabbit whole blood and physiological saline were taken and mixed with 1 : 1.25 volume ratio. The SF films were cut into square pieces 5 mm × 5 mm in size, put into a beaker, washed with deionized water three times, and immersed into physiological saline for 30 min. The cleaned films were put into the bottom of the test tube and 10 mL physiological saline was added. The test tube was put into constant temperature water bath at 37°C for half an hour. Subsequently, 0.2 mL previously prepared diluted rabbit whole blood was added, gently shaken, and placed in constant temperature water bath at 37°C for 1 hour. The positive and negative controls were produced by adding 0.2 mL of diluted rabbit whole blood to 10 mL of deionized water and physiological saline, respectively. Next, all the samples were centrifuged at 1500 rpm for 10 min. The absorbance of the supernatant liquid was measured at 545 nm using an ultraviolet spectrophotometer [25]. The hemolysis rate was calculated as follows:

$$\text{Hemolysis rate} = \frac{(\text{AS} - \text{AN})}{(\text{AP} - \text{AN})}, \quad (2)$$

where AS denotes the absorbance of the sample to be tested; AP denotes the absorbance of positive control; and AN denotes the absorbance of negative control.

3. Results and Discussion

3.1. The Optimal UV-Light Conditions. In $LiBr/ZnCl_2$ DES, the anticoagulant properties of SF films were investigated under different UV-light conditions, as shown in Table 2. The different wavelength bands and irradiation times have different effects on the anticoagulant properties of SF films. Compared with other conditions, under the UV-light region of 254 nm and the irradiation time of 6 h, the anticoagulant properties of SF films were the best, specifically, the recalcification time was 182 s and the hemolysis rate was 3.93%. The anticoagulant properties of SF films were reduced under the lower UV-light energy and shorter UV-light irradiation time; the reason may be that the hydrophilicity and roughness of the films did not change obviously due to low light energy and short time. In addition, there was no further test of 7 h irradiation time because of the high UV-light irradiation energy. The side chain of SF will be broken after long time of irradiation, and then the main chain will also be oxidized and degraded [26]. The anticoagulant properties of SF films can be improved by the proper amount of UV-light irradiation. Therefore, the UV-light conditions for SF films with optimal anticoagulant properties were 254 nm light source wavelength, 11 cm light source distance, and 6 h irradiation time.

3.2. Effects of $LiBr/ZnCl_2$ DES and UV-Light on Anticoagulant Properties of SF Films. In $LiBr/ZnCl_2$ DES, SF films were prepared using UV-light and non-light methods, and the anticoagulant properties of SF films were studied. As shown in Figure 1, under non-light irradiation, the recalcification time of SF films was 129 s, the BCI value of SF films was decreased to close to 0 at 60 min (the higher BCI value indicates the stronger ability of the material to inhibit thrombosis [27]), and the hemolysis rate of SF films was 7.90% (only when the hemolysis rate of biofilms is no more than 5%, can it meet the medical requirements [12]). After UV-light irradiation, the recalcification time of SF films was 182 s, the BCI of the SF films remained at a high level at 60 min, and the hemolysis rate of SF films was 3.93%. It can be seen that through $LiBr/ZnCl_2$ DES, the plasma recalcification time of SF films was increased by 19 s compared with normal blood, but hemolysis rate did not meet the medical requirements. Compared with SF films under non-light irradiation, after UV-light irradiation, recalcification time was prolonged by 53 s, the BCI of the SF films was much higher when the time was 5 min and the overall decline rate was slow, and the hemolysis rate of SF films met the medical requirements.

The anticoagulant properties of SF films were improved mainly due to the changes of hydrophilicity and roughness of the films, which were characterized by contact angle and AFM. It can be seen from Figure 2(a) that under non-light irradiation, the contact angle of SF films was 83.55°. After UV-light irradiation, the contact angle of SF films was 66.50°. The results showed that the hydrophilicity of SF films was increased through $LiBr/ZnCl_2$ DES (compared with $CaCl_2$-C_2H_5OH-H_2O three-system salt solution [8]) and improved greatly after UV-light irradiation. The reason for this change may be that the number of hydrophilic groups on the surface of SF films was increased after UV-light irradiation. In addition, the surface roughness of SF films was observed by AFM. As shown in Figure 2, after UV-light irradiation, the morphology of SF films was more orderly, and the roughness of SF films was significantly reduced.

Next, the structural changes of SF films were characterized by XRD. In XRD spectroscopy (Figure 3), under non-light irradiation, diffraction peaks were observed at $2\theta = 18.2°$, 19.7°, and 24.7° corresponding to α-helix conformation. After UV-light irradiation, diffraction peak was observed at $2\theta = 20.7°$ corresponding to β-sheet conformation and diffraction peaks were observed at $2\theta = 28.4°$, 24.7° corresponding to α-helix conformation. In the FTIR (Figure 3), under non-light irradiation, two characteristic vibrational bands were observed at 1650 cm^{-1} (amide I) and 1538 cm^{-1} (amide II) corresponding to the α-helix structure of SF and a characteristic vibration band was observed at 1265 cm^{-1} (amide III) corresponding to the β-sheet structure of SF. After UV-light irradiation, two characteristic vibrational bands were observed at 1616 cm^{-1} (amide I) and 1515 cm^{-1} (amide II) corresponding to the β-sheet structure of SF and a characteristic vibration band was observed at 1236 cm^{-1} (amide III) corresponding to the α-helix structure of SF. The amide I and amide II bands of SF films prepared under UV-light irradiation moved from 1650 cm^{-1} and 1538 cm^{-1} to 1616 cm^{-1} and 1515 cm^{-1}, respectively. It can be seen from the above that the conformation of SF films changed from α-helix to β-sheet structure after UV-light irradiation.

From the above analysis, UV-light irradiation and $LiBr/ZnCl_2$ DES have synergistic effect on improving the anticoagulant properties of SF films. This may be because under the synergistic effect of UV-light irradiation and $LiBr/ZnCl_2$ DES, on the one hand, the secondary structure of SF films changed α-helix to β-sheet, and the hydrophilicity of SF films was enhanced; on the other hand, the surface roughness of SF films was reduced. It has been reported that high hydrophobicity and roughness on the surface of the films will lead to the increase of available surface area, which makes more plasma proteins adhere to the surface of the films and results in blood coagulation [28, 29]. Therefore, the adsorption of plasma protein on the surface of SF films was reduced through the enhancement of hydrophilicity and the reduction of surface roughness, so the blood coagulation time was prolonged and the anticoagulant properties of SF films were enhanced [21, 30].

Table 2: Recalcification time and hemolysis rate of SF films under different UV-light conditions.

Wavelength (nm)	Distance (cm)	Time (h)	Recalcification time (s)	Hemolysis rate (%)
254	11	5	170	4.17
		6	182	3.93
295		6	165	4.20
365		5	164	4.80

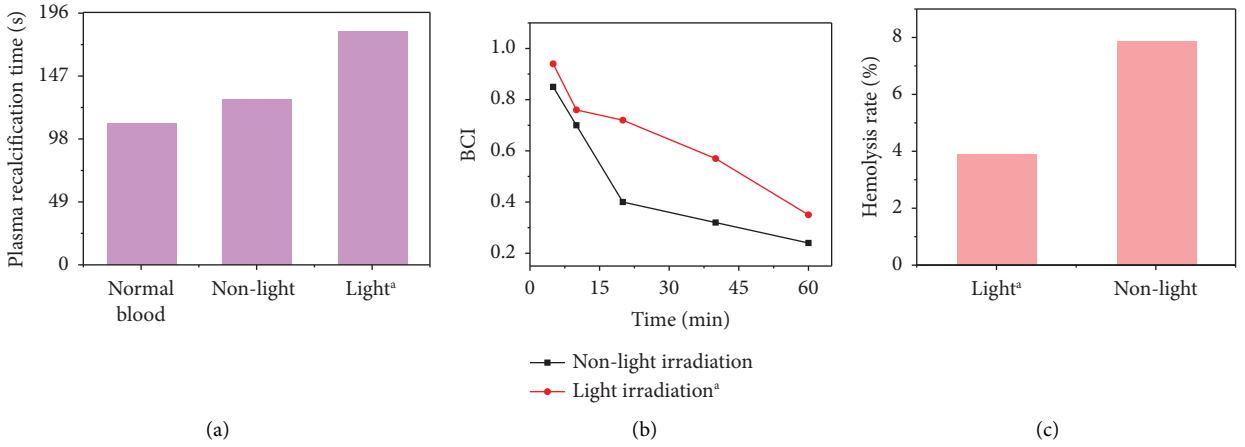

Figure 1: (a) Plasma recalcification time. (b) BCI. (c) Hemolysis rate of SF films under different conditions. [a]Irradiation conditions: UV-light from xenon lamp at 254 nm; 11 cm from light source; irradiation time of 6 h.

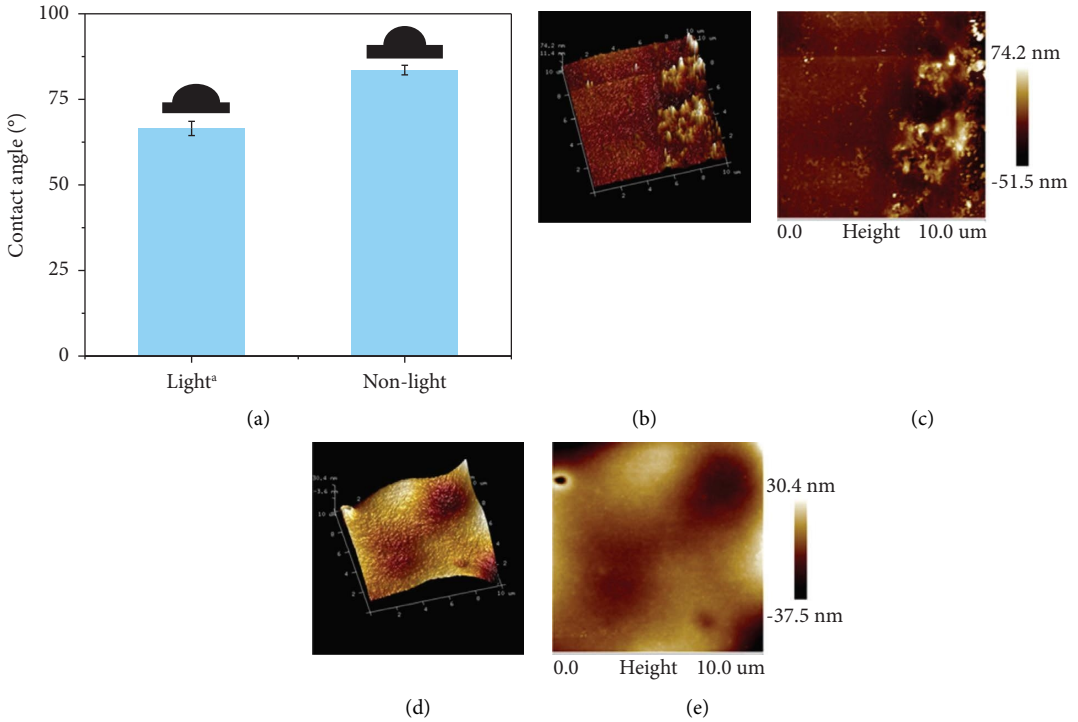

Figure 2: (a) Contact angle. (b, c) AFM on non-light irradiation. (d, e) AFM on UV-light irradiation of SF films under different conditions.

3.3. Universality of DES on Anticoagulant Properties of SF Films. Under the optimal UV-light conditions, the anticoagulant properties of SF films were studied in LiBr/urea DES. As shown in Figure 4, the recalcification time of SF films was 176 s, the BCI of SF films remained at a high level at 60 min and the overall decline rate was slow, and the

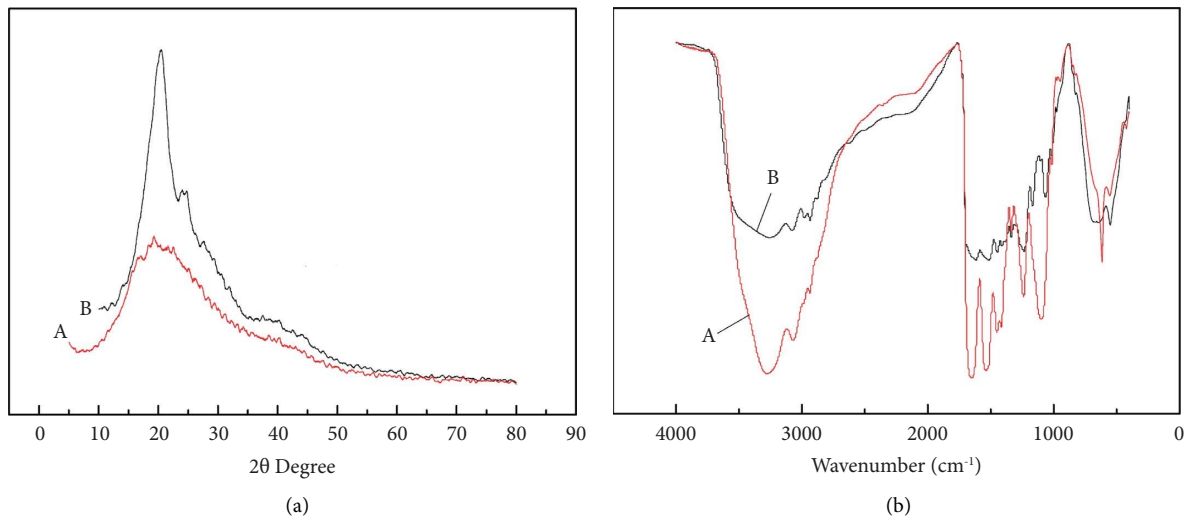

Figure 3: (a) The XRD spectra and (b) the FTIR spectra of SF films under different conditions: (A) non-light irradiation; (B) UV-light irradiation.

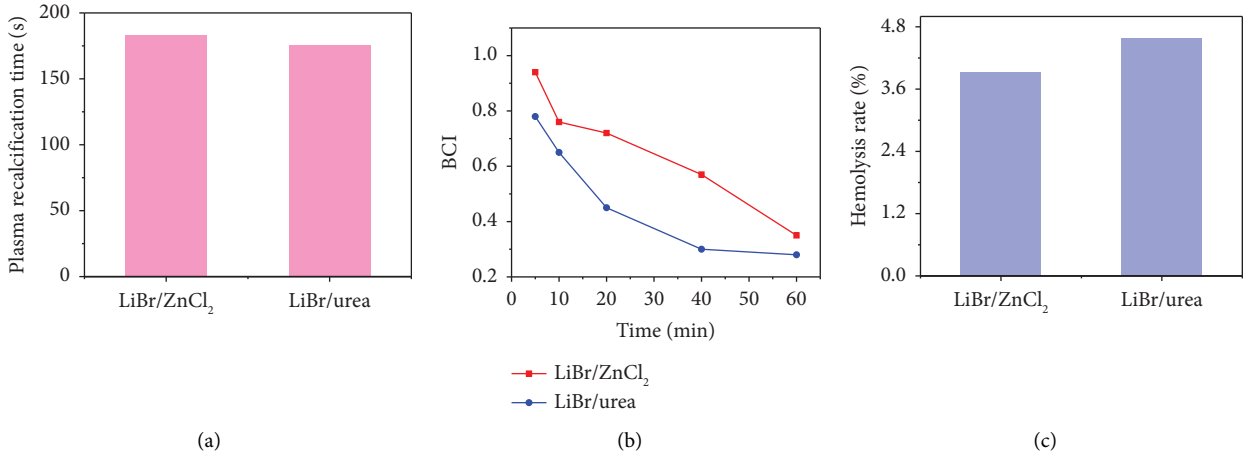

Figure 4: (a) Plasma recalcification time. (b) BCI. (c) Hemolysis rate of SF films under different DESs on the optimal UV-light conditions.

hemolysis rate of SF films was 4.56%. It can be seen that the plasma recalcification time of SF films was increased by 15 s through the effects of LiBr/urea DES, which was similar to that of $LiBr/ZnCl_2$ DES.

In addition, the structure changes of SF films were characterized in LiBr/urea DES, as shown in Figure 5. In the FTIR, after optimal UV-light irradiation, two characteristic vibrational bands were observed at 1639 cm^{-1} (amide I) and 1513 cm^{-1} (amide II) corresponding to the β-sheet structure of SF and a characteristic vibration band was observed at 1235 cm^{-1} (amide III) corresponding to the α-helix structure of SF. The results showed that the amide I and amide II bands of SF films moved from 1650 cm^{-1} and 1538 cm^{-1} to 1639 cm^{-1} and 1513 cm^{-1} after the optimal UV-light irradiation. Next, it can be further seen from XRD that after optimal UV-light irradiation, diffraction peaks were observed at $2\theta = 18.9$ and 40.0° corresponding to β-sheet conformation and diffraction peak was observed at $2\theta = 24.7^{\circ}$ corresponding to α-helix conformation. A new high intensity diffraction peak appeared at $2\theta = 18.9^{\circ}$ after UV-light irradiation, which was attributed to the characteristic peak of β-sheet. The results showed that the secondary structure of SF was transformed from α-helix to β-sheet after UV-light irradiation. Moreover, it can be seen in Figure 6 that the hydrophilicity and roughness of SF films were improved greatly after UV-light irradiation, which were similar to that of $LiBr/ZnCl_2$ DES.

Hence, although $ZnCl_2$ and urea are structurally different, they can form DES by hydrogen bonding with LiBr. Under the optimum UV-light conditions, these two DESs have universality to enhance the anticoagulant properties of SF films, which was mainly because under the synergistic effect of DES and UV-light, on the one hand, the hydrophilicity of SF films was improved, and the adsorption of blood components is effectively prevented; on the other hand, the roughness of the SF films was decreased, which was not conducive to the absorption of

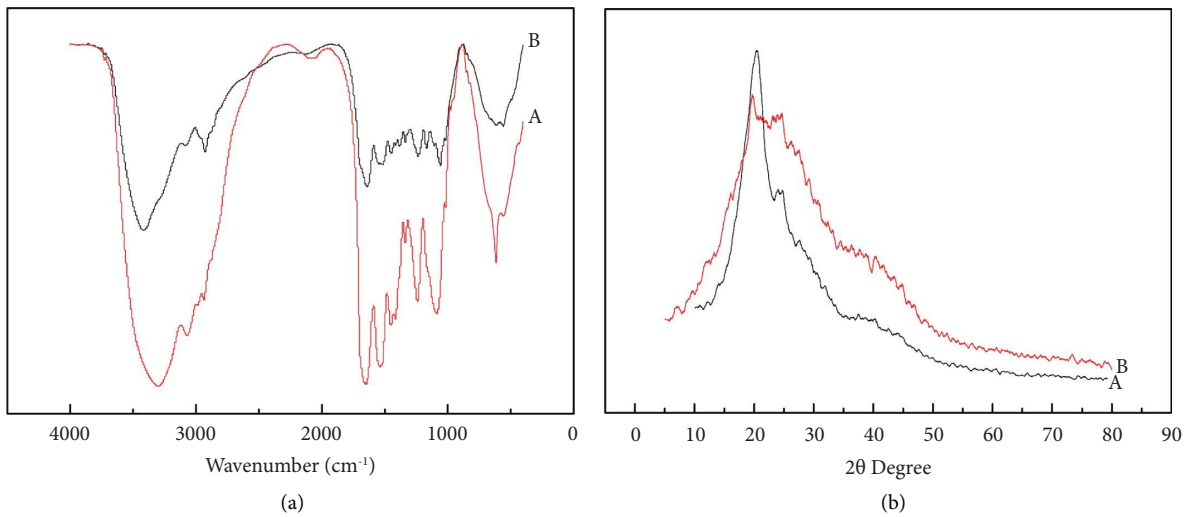

Figure 5: The FTIR (a) and XRD (b) spectra of SF films using LiBr/urea DES under different conditions: (A) non-light irradiation; (B) UV-light irradiation.

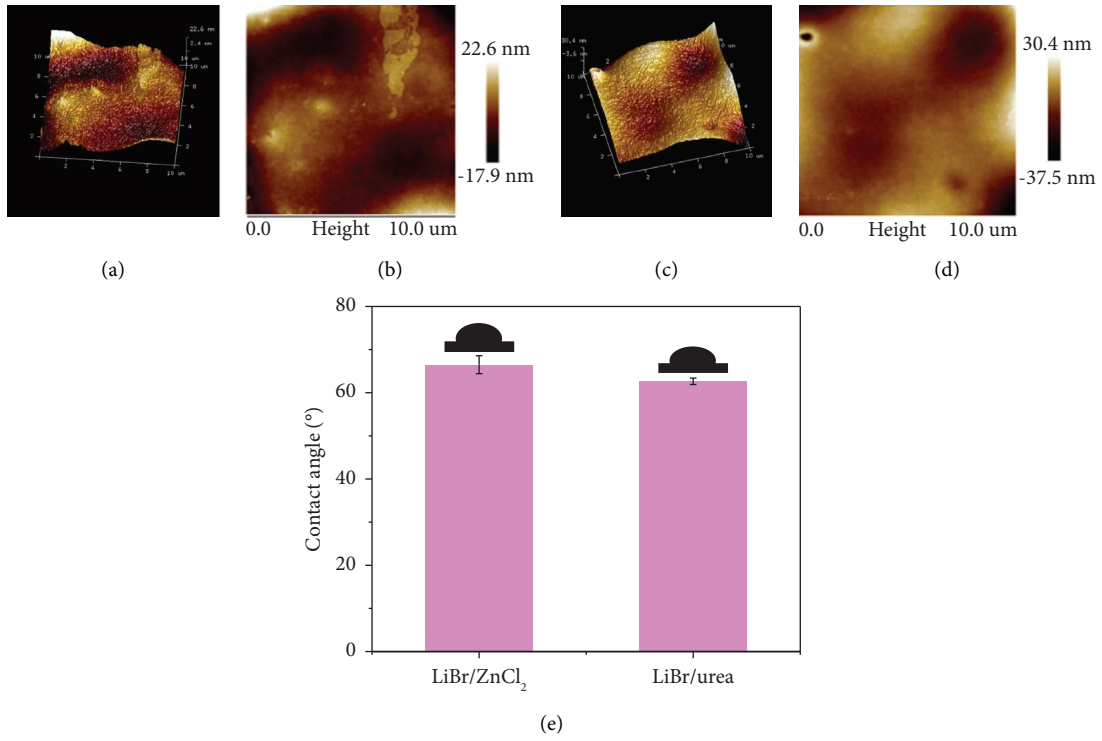

Figure 6: The roughness of SF films under different DESs ((a, b) LiBr/urea; (c, d) LiBr/$ZnCl_2$) on the optimal UV-light conditions. (e) The hydrophilicity of SF films under different DESs on the optimal UV-light conditions.

blood components, and the blood was not easy to coagulate, and thus the anticoagulant properties of SF films were enhanced.

4. Conclusion

A novel SF film with strong anticoagulant properties was fabricated through the synergistic effect of DES and UV-light irradiation. Its excellent anticoagulant properties expand the application range of SF films. This study offers a novel concept for the preparation of strong anticoagulant SF films that can be extended to the preparation of other polymer materials.

Data Availability

The data used to support the findings of this study are included within the article.

Conflicts of Interest

The authors declare that they have no conflicts of interest.

Acknowledgments

This research was supported by the National Science Foundation of China (grant nos. 31670594 and 21908124), the Qingdao People's Livelihood Plan (17-3-3-83-nsh), the Key R&D Project of Shandong (2017GGX40106), and the Taishan Scholar Program of Shandong (grant no. 201511033).

References

[1] T. Aper, M. Wilhelmi, C. Gebhardt et al., "Novel method for the generation of tissue-engineered vascular grafts based on a highly compacted fibrin matrix," *Acta Biomaterialia*, vol. 29, pp. 21–32, 2016.

[2] P. G. Shi, L. Zhang, W. Tian et al., "Preparation and anticoagulant activity of functionalised silk fibroin," *Chemical Engineering Science*, vol. 199, pp. 240–248, 2019.

[3] Y. Tamada, "Sulfation of silk fibroin by chlorosulfonic acid and the anticoagulant activity," *Biomaterials*, vol. 25, no. 3, pp. 377–383, 2004.

[4] B. D. Ratner, "The catastrophe revisited: blood compatibility in the 21st century," *Biomaterials*, vol. 28, no. 34, pp. 5144–5147, 2007.

[5] T. E. Warkentin, M. N. Levine, J. Hirsh et al., "Heparin-induced thrombocytopenia in patients treated with low-molecular-weight heparin or unfractionated heparin," *New England Journal of Medicine*, vol. 332, no. 20, pp. 1330–1336, 1995.

[6] M. Cestari, V. Muller, C. V. Nakamura, A. F. Rubira, and E. C. Muniz, "Preparing silk fibroin nanofibers through electrospinning: further heparin immobilization toward hemocompatibility improvement," *Biomacromolecules*, vol. 15, no. 5, pp. 1762–1767, 2014.

[7] H. F. Liu, X. M. Li, G. Zhou, H. B. Fan, and Y. B. Fan, "Electrospun sulfated silk fibroin nanofibrous scaffolds for vascular tissue engineering," *Biomaterials*, vol. 32, no. 15, pp. 3784–3793, 2011.

[8] K. Wei, B. S. Kim, K. Abe, G. Q. Chen, and I. Kim, "Fabrication and fibroblast attachment property of regenerated silk fibroin/tetramethoxysilane nanofibrous biocomposites," *Advanced Engineering Materials*, vol. 14, no. 5, pp. B258–B265, 2012.

[9] T. P. Zhou, H. Shan, H. Yu et al., "Nanopore Confinement of electrocatalysts optimizing triple transport for an ultrahigh-power-densityzinc-air fuel cell with robust stability," *Advanced Materials*, vol. 32, no. 47, Article ID 2003251, 2020.

[10] N. Zhang, T. P. Zhou, J. K. Ge et al., "High-density planar-like Fe_2N_6 structure catalyzes efficient oxygen reduction," *Matter*, vol. 3, no. 2, pp. 509–521, 2020.

[11] X. X. Yu, T. P. Zhou, J. K. Ge, and C. Z. Wu, "Recent advances on the modulation of electrocatalysts based on transition metal nitrides for the rechargeable Zn-Air battery," *ACS Materials Letters*, vol. 2, no. 11, pp. 1423–1434, 2020.

[12] W. J. Yuan, Y. K. Feng, H. Y. Wang et al., "Hemocompatible surface of electrospun nanofibrous scaffolds by ATRP modification," *Materials Science and Engineering: C*, vol. 33, no. 7, pp. 3644–3651, 2013.

[13] X. M. Yu, Z. Xiong, J. L. Li, Z. Y. Wu, Y. Z. Wang, and F. Liu, "Surface PEGylation on PLA membranes via microswelling and crosslinking for improved biocompatibility/hemocompatibility," *RSC Advances*, vol. 5, no. 130, pp. 107949–107956, 2015.

[14] S. Thi and K. M. Lee, "Comparison of deep eutectic solvents (DES) on pretreatment of oil palm empty fruit bunch (OPEFB): cellulose digestibility, structural and morphology changes," *Bioresource Technology*, vol. 282, pp. 525–529, 2019.

[15] S. L. Liu, Q. Zhang, S. H. Gou, L. L. Zhang, and Z. G. Wang, "Esterification of cellulose using carboxylic acid-based deep eutectic solvents to produce high-yield cellulose nanofibers," *Carbohydrate Polymers*, vol. 251, Article ID 117018, 2021.

[16] M. Esmaeili, I. Anugwom, M. Mänttäri, and M. Kallioinen, "Utilization of DES-Lignin as a bio-based hydrophilicity promoter in the fabrication of antioxidant polyethersulfone membranes," *Membranes*, vol. 8, no. 3, p. 80, 2018.

[17] M. A. Fadel, N. A. Kamel, S. L. Abd El-Messieh, K. N. Abd-El-Nour, and W. A. Khalil, "Ultraviolet surface modification of polyethylene terephthalate (PET) for reducing thrombogenicity," *KGK-Kautschuk Gummi Kunststoffe*, vol. 72, pp. 34–39, 2019.

[18] C. X. Xie, W. J. Li, Q. Q. Liang, S. T. Yu, and L. Li, "Fabrication of robust silk fibroin film by controlling the content of β-sheet via the synergism of UV-light and ionic liquids," *Applied Surface Science*, vol. 492, pp. 55–65, 2019.

[19] H. L. Zhu, X. X. Feng, H. P. Zhang, Y. H. Guo, J. Z. Zhang, and J. Y. Chen, "Structural characteristics and properties of silk fibroin/poly(lactic acid) blend films," *Journal of Biomaterials Science, Polymer Edition*, vol. 20, no. 9, pp. 1259–1274, 2009.

[20] Y. Z. Liao, L. H. Li, J. Chen et al., "Tailoring of TiO_2 films by H_2SO_4 treatment and UV irradiation to improve anticoagulant ability and endothelial cell compatibility," *Colloids and Surfaces B: Biointerfaces*, vol. 155, pp. 314–322, 2017.

[21] A. T. Neffe, M. von Ruesten Lange, S. Braune et al., "Poly(ethylene glycol) grafting to poly(etherimide) membranes: influence on protein adsorption and thrombocyte adhesion," *Macromolecular Bioscience*, vol. 13, no. 12, pp. 1720–1729, 2013.

[22] A. B. Tesler, B. M. Maoz, Y. Feldman, A. Vaskevich, and I. Rubinstein, "Solid-state thermal dewetting of just-percolated gold films evaporated on glass: development of the morphology and optical properties," *Journal of Physical Chemistry C*, vol. 117, no. 21, pp. 11337–11346, 2013.

[23] D. W. Jin, J. F. Hu, D. K. Xia et al., "Evaluation of a simple off-the-shelfbi-layered vascular scaffold based on poly(L-lactide-co-ε-caprolactone)/silk fibroin in vitro and in vivo," *International Journal of Nanomedicine*, vol. 14, pp. 4261–4276, 2019.

[24] T. Y. Zhao, H. Zhang, P. Li, and J. S. Liang, "Effect of tourmaline nanoparticles on the anticoagulation and cytotoxicity of poly(L-lactide-co-caprolactone) electrospun fibrous membranes," *RSC Advances*, vol. 9, no. 2, pp. 704–710, 2019.

[25] Y. Li, J. Li, T. H. Liu et al., "Preparation and antithrombotic activity identification of Perinereis aibuhitensis extract: a high temperature and wide pH range stable biological agent," *Food & Function*, vol. 8, no. 10, pp. 3533–3541, 2017.

[26] J. W. Yin, Y. Duan, and Z. Z. Shao, "UV induced superhydrophilicity of RSF film," *Acta Chimica Sinica*, vol. 72, no. 1, pp. 51–55, 2014.

[27] Q. He, Q. Ao, K. Gong et al., "Preparation and characterization of chitosan-heparin composite matrices for blood

contacting tissue engineering," *Biomedical Materials*, vol. 5, Article ID 055001, 2010.

[28] J. Zhao, L. C. Bai, K. Muhammad et al., "Construction of hemocompatible and histocompatible surface by grafting antithrombotic peptide ACH_{11} and hydrophilic PEG," *ACS Biomaterials Science & Engineering*, vol. 5, no. 6, pp. 2846–2857, 2019.

[29] S. Braune, M. Lange, K. Richau et al., "Interaction of thrombocytes with poly(ether imide): the influence of processing," *Clinical Hemorheology and Microcirculation*, vol. 46, no. 2-3, pp. 239–250, 2010.

[30] C. C. Shi, W. J. Yuan, M. Khan et al., "Hydrophilic PCU scaffolds prepared by grafting PEGMA and immobilizing gelatin to enhance cell adhesion and proliferation," *Materials Science and Engineering: C*, vol. 50, pp. 201–209, 2015.